CrossMark

J. Plasma Physics (2015), *vol.* 81, 395810404 © Cambridge University Press 2015. This is an Open Access article, distributed under the terms of the Creative Commons Attribution licence (http://creativecommons.org/licenses/by/3.0/), which permits unrestricted re-use, distribution, and reproduction in any medium, provided the original work is properly cited.

doi:10.1017/S0022377815000483

Self-organized braiding in solar coronal loops

M. A. Berger[1]†, M. Asgari-Targhi[2] and E. E. DeLuca[2]

[1]CEMPS, University of Exeter, EX4 4QF, UK
[2]Harvard-Smithsonian Center for Astrophysics, 60 Garden Street MS-15, Cambridge, MA 02138, USA

(Received 12 November 2014; revised 9 April 2015; accepted 9 April 2015; first published online 2 June 2015)

In this paper, we investigate the evolution of braided solar coronal loops. We assume that coronal loops consist of several internal strands which twist and braid about each other. Reconnection between the strands leads to small flares and heating of the loop to x-ray temperatures. Using a method of generating and releasing braid structure similar to a forest fire model, we show that the reconnected field lines evolve to a self-organised critical state. In this state, the frequency distributions of coherent braid sequences as well as flare energies follow power law distributions. We demonstrate how the presence of net helicity in the loop alters the distribution laws.

1. Introduction

It was realised many years ago that the solar corona is some 200 times hotter than the underlying photosphere. This has been puzzling scientists for decades. The energy required for the heating of the corona and the detailed physical processes that result in the heating of the corona are not yet accurately and fully understood. It is clear from the observations and modelling that magnetic fields play an important role in the heating process (Schrijver and Zwaan 2000; Aschwanden 2004; Golub and Pasachoff 2009).

The two main theories of coronal heating are stressing models and wave heating models (Ionson 1985; Milano et al. 1997; Mandrini et al. 2000). In the magnetic stress or direct current (DC) heating models, the energy is dissipated within the coronal magnetic fields stressed by slow random footpoint motions. In wave- or alternating current (AC) models, photospheric footpoint motions generate magnetohydrodynamics (MHD) waves that propagate upward along the magnetic flux tubes, and dissipate their energy in the corona. In both types of heating mechanisms, the footpoint motions play an important role in constructing the complex structure needed to create the heating in the corona. The footpoint motions are caused by interactions of granule and supergranule convective flows with magnetic flux elements at the photosphere.

The major difference between DC and AC models concerns the timescale τ_f of the footpoint motions in comparison to the coronal Alfvén travel time $L_{\rm cor}/v_A$, where $L_{\rm cor}$ is the coronal loop length and v_A the coronal Alfvén speed. When $\tau_f \gg L_{\rm cor}/v_A$, the corona responds quasi-statically to the footpoint motions, allowing the build up of magnetic stresses within the coronal field lines. When this stress reaches a critical

† Email address for correspondence: m.berger@exeter.ac.uk

https://doi.org/10.1017/S0022377815000483 Published online by Cambridge University Press

value, the magnetic energy is released resulting in the heating of the corona. In contrast, in wave heating models, where $\tau_f < L_{\rm cor}/v_A$, the time scale of the wave excitation is smaller than the Alfvén wave travel time. Therefore, the waves will bounce back and forth within the coronal structure creating wave like responses to the footpoint motions (van Ballegooijen et al. 2014).

van Ballegooijen et al. (2011) recently developed a three-dimensional (3D) MHD model describing the propagation and dissipation of Alfvén waves in active region loops (also see (Asgari-Targhi and van Ballegooijen 2012; Asgari-Targhi et al. 2013, 2014; van Ballegooijen et al. 2014)). This model includes a detailed description of Alfvén waves in the coronal part of the loop, as well as in the lower atmospheres at the two ends of the loop. The focus of this research is to determine how coronal loops with temperatures in the range 1–3 MK are heated. The Alfvén wave turbulence model provides the energy needed to heat coronal magnetic field lines with this temperature range. Also, the observational signatures of the Alfvén wave turbulence model are consistent with measurements of the non-thermal line broadenings from the Extreme-Ultraviolet Imaging Spectrometer (EIS) (Asgari-Targhi et al. 2014). Although the Alfvén wave turbulence is a plausible theory for explaining the heating of coronal loops observed in the AIA 171 channel, the challenge remains as to whether the wave turbulence model can explain the hot plasma that features in the loops with temperature more than 5 MK (Asgari-Targhi et al. 2015). Thus, it is useful to consider another mechanism that could explain the heating of hot loops (>5 MK), magnetic reconnection.

An example of the DC heating mechanism is given by the magnetic braiding model (Parker 1972, 1983; Berger 1993; Berger and Asgari-Targhi 2009). The picture of coronal heating considered by Parker describes a highly conducting coronal plasma evolving due to slow, random footpoint motions. In this model, it is assumed that the corona responds quasi-statically to the footpoint motions. Therefore, it maintains an equilibrium which gradually adjusts as its topology changes. A random walk of the footpoints causes tangling and braiding of the coronal field lines.

Parker (1972) proposed that the complex topology of the braided field leads to the formation of tangential discontinuities; smooth equilibria fail to exist and electric current sheets form (also see Ng and Bhattacharjee 1998; Janse and Low 2009; Craig 2010; Janse et al. 2010; Low 2010).These current layers might burn in a series of fast reconnection events known as 'nanoflares' (Parker 1988). A rigorous proof that true current discontinuities form in sufficiently complex topologies remains elusive, but numerical experiments show that very thin current layers will certainly form Wilmot-Smith et al. (2009, 2011).

In some versions of the braiding model, the reconnection switches on when the misalignment angle between neighbouring flux tubes reaches a critical value (Parker 1988; Berger 1993; Dahlburg et al. 2005), in other versions the reconnection occurs even for small angles (van Ballegooijen 1986). The response of coronal loops to nanoflares has been studied in great detail (e.g. Cargill and Klimchuk 1997; Winebarger and Warren 2005; Patsourakos and Klimchuk 2006; Klimchuk et al. 2008; Reep et al. 2013), leading to a common view that solar active regions may be heated by nanoflare storms. Magnetic braiding may also determine the widths of coronal loops (Schrijver 2007; Galloway et al. 2006).

In order to release enough energy to heat the corona, the reconnection must be delayed. Delaying rapid reconnection allows the build up of substantial energy reserves in the magnetic field lines. As the magnetic field becomes more and more braided and twisted, its energy will generally increase quadratically in time (Parker 1983;

https://doi.org/10.1017/S0022377815000483 Published online by Cambridge University Press

Berger 1991, 1993). If reconnection occurs too early, there will not be enough energy stored to power flares or coronal heating. This picture has run into some difficulties. First, the main assumption in Parker's analysis is that coronal magnetic flux tubes must be wrapped around each other over a period of many hours, i.e. the flux tubes must retain their identity for a long time. This assumption is questionable because observations show that photospheric flux elements continually split up and merge on a time scale of a few minutes (Berger and Title 1996; Cirtain et al. 2013). After a flux element breaks up, the individual fragments disperse as a consequence of turbulent motions below the photosphere. If two or more neighbouring flux elements break up, the individual fragments will move around with granular motion and will be swept into the edges of granules or supergranules. Eventually, the fragments coalesce into new flux concentrations that will generally have a different mixture of flux fragments from the old flux elements. This process of splitting and merging will increase the topological complexity of the overlying coronal field. It is not clear what effect this will have on the process of coronal heating. Berger (1994) proposed that the increased complexity of the coronal field will contribute to the heating of the coronal loops. Another possibility is that the added complexity causes the magnetic free energy of the braided field to be released too early, which lowers the energy input rate; the predicted heating rate may then be insufficient to explain the observed heating (van Ballegooijen 1986). Therefore, at present it is unclear whether quasi-static braiding models can provide sufficient energy in active regions.

In this paper, using the braiding model of Parker, we consider coronal loops as braided fields between two parallel plates. The footpoint motions are applied at these boundary plates. Although in the real Sun, these motions will undergo change in their velocity amplitude from 1–2 km s^{-1} at the photosphere to about 15–40 km s^{-1} in the corona (Asgari-Targhi et al. 2014), here we solely concentrate on the topological structure of the field lines and do not ascribe this velocity variation from photosphere to the corona to our braided field lines. For the purpose of our analysis, we assume that the field lines are divided into discrete flux elements and there is no fragmentation or interactions between these field lines, except in discrete reconnection events. This greatly simplifies the geometry of the field lines while it captures the large scale geometry of the tangled magnetic field. As stated in our previous paper (van Ballegooijen et al. 2014), this quasi-static model of coronal heating is unrealistic and like many similar quasi-statics modelling of coronal loops, ignores the coupling between the photosphere and corona over many density scale heights. However, since the aim of this paper is to present statistical evidence of the distribution of energy release within the coronal field lines, we focus mainly on the geometry of these field lines.

The plan of this paper is as follows. Section 2 provides a review on the power law distribution of flare energies. In Sec. 3, we construct the algebraic model of the braided structure within magnetic flux elements and present our results. Discussion and conclusion are given in Sec. 4.

2. Power aw distribution of solar flares

Solar flares are very energetic phenomena where magnetic reconnection results in large amounts of energy being dissipated by the heating of thermal plasma and acceleration of high energy particles. Solar flares are thought to have energies ranging from $<10^{26}$ ergs to 10^{33} ergs. Microflares and nanoflares occur at a continuous rate and may be responsible for the increase in the energy of the hot plasma in the solar coronal loops. Observations of solar flares in all wavelengths indicate that the

https://doi.org/10.1017/S0022377815000483 Published online by Cambridge University Press

distribution of the flare peak intensities follow a power law (Datlowe et al. 1974; Lin et al. 1984; Dennis 1985; Einaudi and Velli 1999; Charbonneau et al. 2001; Hudson 2010; Aschwanden 2013):

$$P(E) \sim E^{-\alpha}. \tag{1}$$

The power law slope varies over a range of $\alpha \approx 1.1$–2.8 in different wave lengths. The power law index of the distribution is independent of solar cycle. Lu and Hamilton (1991) make a direct connection between power law dependence of the flare occurrence rate and the flare size. They suggest that the solar magnetic field provides an example of self-organised criticality.

In order to explain the prevalence of power-law correlations extending over many decades in complex dynamical systems, Bak et al. (1987, 1988) proposed the concept of self-organised criticality. In their modelling, they show that extended systems with many metastable states can naturally evolve into a critical state with no intrinsic scale. Numerical simulations (Carlson and Langer 1989; Kadanoff et al. 1989) as well as experiments (Babcock and Westervelt 1990) demonstrate the existence of such critical states. Examples of self-organised critical models are forest fire and avalanche models. In a forest fire model, isolated clumps of trees can be destroyed by a fire caused, for example, by a lightning strike. The loss of trees due to fire is balanced by the birth and growth of new trees at random positions. Over time, small clumps of trees emerge as neighbouring positions fill with new trees. Smaller clumps can merge to become larger clumps, until a lightning strike hits. A critical state is eventually reached with a statistically stable distribution of clump and fire sizes.

A simple example of an avalanche model is a sand pile or snowfield on a mountainside. If small sections of the snow are too steep, a mini-avalanche will occur. Mini-avalanches will sometimes trigger large avalanches, which then may trigger even larger avalanches. Meanwhile, new snow falls onto the mountainside. As the snow accumulates, the average slope of the pile or mountainside increases, until a critical state is reached, where avalanches balance the addition of new material.

In these models, the critical state is found to be insensitive to initial conditions. Furthermore, it does not require any fine tuning of parameters. The system becomes stationary when the perturbations cause disturbances that are able to propagate the length of the system. Once the system is in a critical state, it has a distribution of minimally stable regions of all sizes. Therefore, small perturbations give rise to avalanches of all sizes from the smallest possible avalanche such as a single sand grain up to the size of the system. A featureless power-law spectrum of avalanche or forest fire sizes results since there is no characteristic length scale in the system.

For a system to exhibit self-organised critical behaviour, a local instability must occur whenever some local parameter exceeds a critical value. This in turn results in a process that changes the value of this quantity at the sites nearby with the possibility of causing the value of the parameter to exceed the critical value at neighbouring sites.

Considering the fact that the corona is heated by many small events, be it bursty heating events as a result of nonlinear interactions between the Alfvén waves in Alfvén wave turbulence model (van Ballegooijen et al. 2011) or nanoflare events, the magnetic field is thought to behave analogous to that of the sandpile and have a local instability, hence can be driven to a self-organised critical state. Lu and Hamilton (1991) suggest that the random twisting of the magnetic field by photospheric convective flows has the same role as the addition of sand grains in a sand pile. In their model, the random photospheric footpoint motions provide the input of energy, and swarms of small

https://doi.org/10.1017/S0022377815000483 Published online by Cambridge University Press

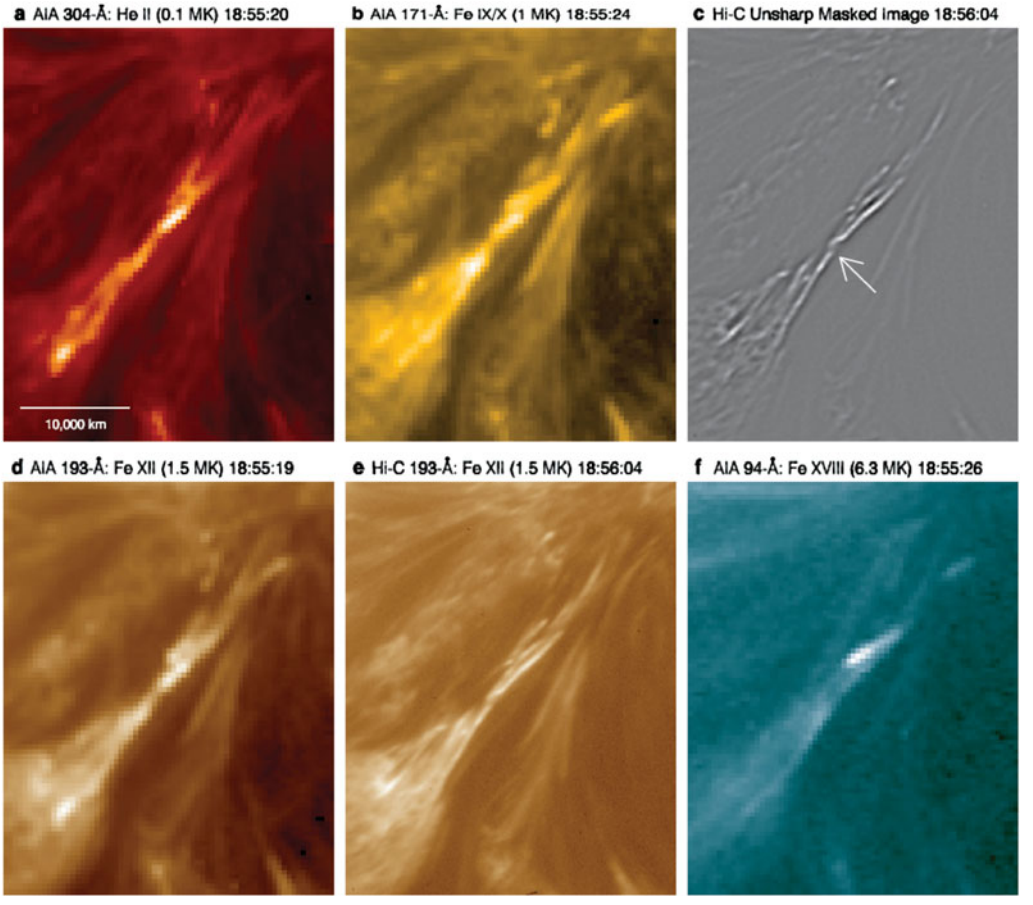

FIGURE 1. Observations of braided filament structures from Hi-C (Cirtain et al. 2013).

flares provide the output. The increase in the magnetic energy excites the flares and these flares trigger more flares in turn in the nearby sites and eventually result in a larger flare. This by no means indicates that the observed flare energy distribution integrates to give sufficient coronal heating. However, there is a possibility that the slope steepens at nanoflare events and steeper slope could mean more small events and hence more heating (Vlahos et al. 1995).

In this paper, using the specific geometry of coronal magnetic field lines, we examine a model reminiscent of forest fire models. Sections of the braid where the twist is all of one sign correspond to the clumps of trees. Reconnection can merge two braid sections. If their helicities are of opposite signs, then they will cancel, releasing energy in the process. In this process, the coronal loops evolve to a self-organised state with power law distribution in energy and twist.

Figure 1 is an image from the High-resolution Coronal Imager (Hi-C) that was launched on a sounding rocket and observed the corona in the 193 Å passband with a spatial resolution of about 0.2 arcs (Cirtain et al. 2013). The authors claim to see highly braided magnetic fields at several locations in the observed active region. Although this image shows the complex structure of solar magnetic strands in a high spatial resolution, it is still difficult to follow individual strands from one end to the other end.

https://doi.org/10.1017/S0022377815000483 Published online by Cambridge University Press

FIGURE 2. A braid with 5 crossings.

3. Generation of braid structure

A braid is a set of curves stretched between two planes. The simplest non-trivial braid consists of two curves twisting about each other. When we look at a braid in projection, we see a certain number of crossings between the individual strings (for example the braid in Fig. 2 has 5 crossings). Suppose a braid has N strings of diameter D and exhibits C crossings. Each crossing will require at least one string to move in a transverse direction. If the strings are magnetic flux tubes, this means that the flux tubes must have a transverse magnetic field $B_\perp$, hence extra magnetic energy. Thus, the magnetic energy increases with the number of crossings. Equations relating magnetic energy to crossing number C are derived in Berger (1993); Berger and Asgari-Targhi (2009).

The theory of braids was first developed by Artin (1947). An algebraic n-braid is a word over the generators of the braid group B_n, that is the set $\{\sigma_i^{\pm 1}\}$ for $1 \leqslant i < n$, where, e.g. σ_2^{-1} gives a negative crossing between the second and third strings from the left. Two words in B_n represent the same braid if, and only if, one can be transformed into the other using the following relations:

$$\sigma_i \sigma_i^{-1} = e, \tag{2}$$

$$\sigma_i \sigma_j = \sigma_j \sigma_i, \tag{3}$$

$$\sigma_i \sigma_{i+1} \sigma_i = \sigma_{i+1} \sigma_i \sigma_{i+1}, \tag{4}$$

where $|i - j| > 1$ and e is the identity in B_n (topologically e is the braid with no crossings; it consists of n vertical strings). The word length for Artin braids equals the number of crossings in a braid. Figure 3 shows an Artin representation of a braid group with three strings.

The diagram in Fig. 3 projects the braid into a plane (for example $x - z$) plane. The strings may be regarded as beginning and ending each crossing lined up parallel to the x-axis, deviating in the y direction only to move around each other. Other projections are also possible, for example onto a cylinder (Berger 1990).

Let us consider three braids in particular. The special braid pattern

$$\Delta = \sigma_1 \sigma_2 \sigma_1 = \sigma_2 \sigma_1 \sigma_2, \tag{5}$$

https://doi.org/10.1017/S0022377815000483 Published online by Cambridge University Press

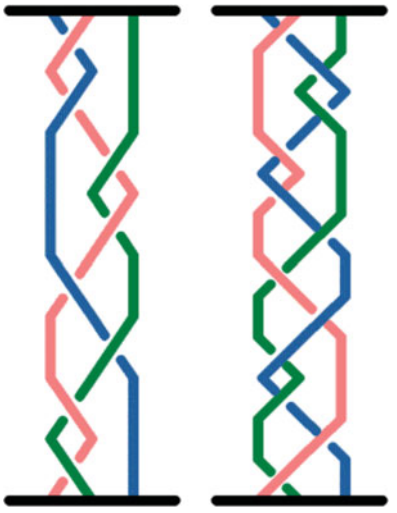

FIGURE 3. Two equivalent braids. On the left, the braid word is (left to right corresponding to bottom to top) $B_1 = \sigma_1^{-2}\sigma_2\sigma_1^{-1}\sigma_2^2\sigma_1^2$, while on the right $B_2 = \sigma_1\sigma_2\sigma_1^2\sigma_2\sigma_1^{-1}\sigma_2\sigma_1^{-2}\sigma_2^{-2}\sigma_1$. Using the braid relations equation (3), one can show that $B_1 \equiv B_2$.

twists the entire braid through half a turn. The square of this, Δ^2 gives a full turn, and commutes with all other braid words in the group (in group theory terminology, powers of Δ^2 constitute the *centre* of the braid group). Half turns *almost* commute with other group elements, in the sense that

$$\Delta\sigma_1 = \sigma_2\Delta\,; \Delta\sigma_2 = \sigma_1\Delta\,. \tag{6}$$

Because the full turns commute with other braid patterns, they can be placed anywhere along the braid. All three braids can be converted to the normal form

$$B = \Delta^n\sigma_1^a\sigma_2^{-b}\sigma_1^c\sigma_2^{-d}. \tag{7}$$

There are several mechanisms which will braid coronal magnetic flux. First, newly emerging flux could already be braided. Secondly, random motions of the footpoints of magnetic strands in a loop will braid the strands above.

Third, a coronal flux tube may be fragmented at its foot points. Imagine that part of a footpoint rotates, twisting the flux above. Then the fragments at the foot point rearrange themselves, and subsequently another part rotates. Even if the second rotation is opposite in sense to the first, the twists generated in the magnetic field do not cancel. The non-cancellation makes random photospheric rotations much more efficient in heating the coronal plasma (Berger 1994). The fragmentation of the footpoints of large coronal loops can be interpreted in terms of the coronal flux connecting to small scale chromospheric loops. These loops can reconnect with each other, leading to an effective motion of the endpoints of the coronal field lines (Priest et al. 2002). Evidence for fragmentation and reconnection near footpoints of coronal loops can be seen in Shibata et al. (2007).

Fourth, reconnection may occur on several scales. Suppose two large bundles of flux reconnect. This has two effects on the smaller flux elements inside. First, their small scale braid patterns are cut in half and reshuffled. Symbolically, if large tube 1 has an internal braid pattern A below the reconnection point and braid pattern B above, and tube 2 has patterns C below and D above, then after reconnection the new tubes will have patterns AD and BC. In addition, when two flux tubes reconnect,

https://doi.org/10.1017/S0022377815000483 Published online by Cambridge University Press

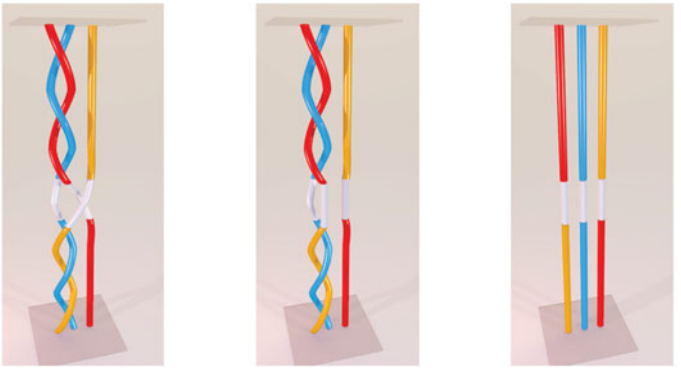

FIGURE 4. An example of a braid pattern where a single reconnection can release all the free energy of the braid. The reconnection site is coloured white. After the right two strands reconnect, negative and positive twist can cancel, thereby releasing their magnetic energy into kinetic energy.

each acquires a half unit of twist (Song and Lysak 1989; Wright and Berger 1989). Thus, the smaller flux elements inside will now twist about each other, adding to the braid patterns additional structure. (Symbolically, if a half twist is represented by the Greek letter Δ, then the final patterns are in fact ΔAD and ΔBC.)

In this paper, we present a model which gives a power law distribution of energy releases. We consider a braid on three strings, with upper boundary fixed. At the lower boundary, braid structure is generated in the strings above by a succession of motions. We suppose at the boundaries the endpoints line up on the x axis. In this model, two motions alternate with each other. The first motion rotates the leftmost and middle endpoints through some net twist angle v, where v is a multiple of π. This generates C crossings in the strings below, where $C = v/\pi$. The sign of C tells us whether the crossing is right-handed or left-handed. The second motion gives a single half twist between the middle and right-hand endpoint. Figure 4 illustrates this. First, the leftmost endpoints rotate through four anti-clockwise half turns ($C = +3$), giving the strings below three positive (right-handed) half twists. Next, the second motion exchanges the third string with the middle string. Finally, a twist of three clockwise turns gives the two strings on the left (no longer the same two strings!) three negative half-twists ($C = -3$). Some descriptive terminology will be useful here. The sections of the braid where the two strings on the left twist about each other will be called *coherent sequences*. The single crossings which swap the middle string with the string on the right will be called *interchanges*. In the above example, there are two coherent sequences with twists $3/2$ and $-3/2$, i.e. $C = +3$ and $C = -3$. Note, however, that the twists cannot cancel because of the interchange.

3.1. *The distribution of twists*

Suppose that, at time t, the braid as a whole has $n(C)$ sequences with crossing number C. At each time step, the model adds one new sequence with δC crossings and one new interchange, while reconnection removes one of the interior interchanges. The twist of the next segment is distributed with probability function $p(\delta C)$.

Say the input is a Poisson process, so that for some λ,

$$p(\delta C) = \frac{\lambda}{2} e^{-\lambda|\delta C|}. \tag{8}$$

https://doi.org/10.1017/S0022377815000483 Published online by Cambridge University Press

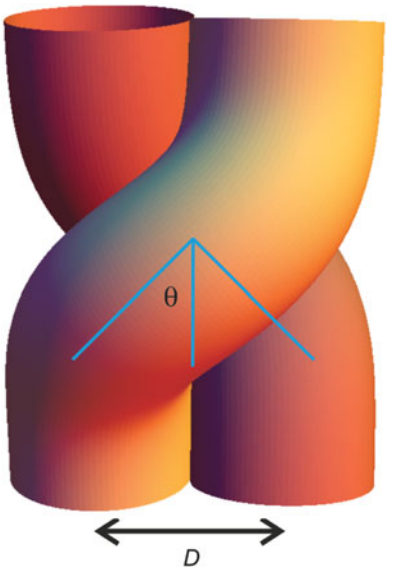

FIGURE 5. Two tubes making a crossing. If the angle of each tube with respect to the vertical is θ, then they will be misaligned by an angle 2θ. To move around each other, each tube must travel a transverse distance of about $\pi D/2$ where D is the diameter of a tube.

One can then find an analytic solution to the steady-state problem, where additions of new sequences balance mergers and cancellations of old sequences (Berger and Asgari-Targhi 2009):

$$n(C) = \frac{\lambda}{2}\left(I_1(\lambda C) - L_{-1}(\lambda C)\right). \tag{9}$$

where I_1 is a Bessel-I function and L_1 is a Struve-L function. The function $n(C)$ closely approximates a power law $n(C) \propto C^{-2}$ for $C \geqslant 3$.

3.2. *The energy distribution*

Let us make a simple estimate of how the transverse field grows with C. Suppose the braided tubes stretch vertically between planes $z = 0$ and $z = L$. We ignore the contribution to the transverse field from the twisting of individual flux elements, i.e. we assume that the transverse field arises predominantly from braiding.

Each crossing involves two strings out of the N strings. Thus, on average, each string takes part in $2C/N$ crossings. This implies a single crossing takes place in a vertical distance of about

$$\delta z = \frac{NL}{2C}. \tag{10}$$

Consider the centre lines of two tubes that rotate about each other between heights z and $z+\delta z$. Assuming the tubes have a circular horizontal cross-section, the transverse distance each tube travels is $\delta\ell = \pi D/2$ (see Fig. 5). Then the typical ratio of transverse field strength to axial field strength will be

$$\frac{B_\perp}{B_\parallel} = \frac{\pi D}{2\delta z} \tag{11}$$

$$= \frac{\pi C D}{NL}. \tag{12}$$

https://doi.org/10.1017/S0022377815000483 Published online by Cambridge University Press

Let $\theta = \tan^{-1} B_\perp / B_\parallel$ give the typical angle of the flux tubes with respect to the vertical. Two crossing flux tubes will be misaligned by as much as twice this angle. When the crossing number becomes large enough, neighbouring tubes will be sufficiently misaligned to trigger reconnection (Linton et al. 2001). If a misalignment of about $\pi/6$ triggers reconnection, then $B_\perp/B_\parallel \approx \tan \pi/12 \approx 0.27$, and the crossing number will be

$$C_{\text{critical}} = \frac{NL}{\pi D} \tan \pi/12 \approx 0.085 \frac{NL}{\pi D}. \tag{13}$$

For flux elements with aspect ratio $L/D = 100$ and $N = 3$, we find $C_{\text{critical}} \approx 25$. We also note that the free energy is proportional to the square of the crossing number. Let

$$E_{\text{free}} = \frac{1}{2\mu} \int B_\perp^2 dv. \tag{14}$$

The volume of the N tubes is approximately $N\pi D^2 L$. Then

$$E_{\text{free}} \approx \frac{N\pi D^2 L}{2\mu} \left(\frac{\pi C D B_\parallel}{NL} \right)^2 = \left(\frac{\pi^3 D^4 B_\parallel^2}{2\mu NL} \right) C^2. \tag{15}$$

The free energy of a set of braided magnetic flux tubes is therefore $E_{\text{free}} = a\, C^2$ where the constant a depends on the length and diameter of the tubes as shown in the above equation.

Suppose that a reconnection reduces the number of crossings from C_{initial} to C_{final}. We define the 'flare energy' to be

$$W = \delta E = a(C_{\text{initial}}^2 - C_{\text{final}}^2). \tag{16}$$

Given the distribution $n(C)$ of coherent sequences, what is the corresponding distribution of flare energies $n(W)$? Berger and Asgari-Targhi (2009) show that $n(W) \propto W^{1-2\alpha}$. For example, if $\alpha = 2$ as in the model of the previous section, then the distribution of flares with energy W decreases as the third power of W, i.e. $n(W) \propto W^{-3}$.

3.3. *Selective reconnection*

A crucial element of our self-organisation models is the hypothesis that reconnection will occur preferentially at certain places along the braid. In other words, a magnetic braid will have weak points where the stresses are largest, and reconnection is most likely to be triggered.

For example, Fig. 4 shows a fairly coherent braid pattern. In the braid on the left, two coherent braid sequences are stacked on top of each other, with one interchange in between. This braid could be generated by a rotational motion at one boundary of one pair of tubes, and at the other boundary by a rotational motion entangling a different pair of tubes. Alternatively, if the motions are at just the lower boundary, the motions could be an anti-clockwise motion of two of the endpoints followed by a clockwise motion with a different pair.

3.4. *Algebraic simulation*

We have run simulations of braids undergoing both random input of crossings at the boundary planes, plus random reconnections in between sequences. We find that initially random braids evolve into a self-critical power law state. Figure 6 shows that the frequency distribution of the sequence size becomes a power law with slope approximately -2, in accord with the analytical results. In this calculation, there were equal probabilities assigned to generating positive sequences and negative sequences.

https://doi.org/10.1017/S0022377815000483 Published online by Cambridge University Press

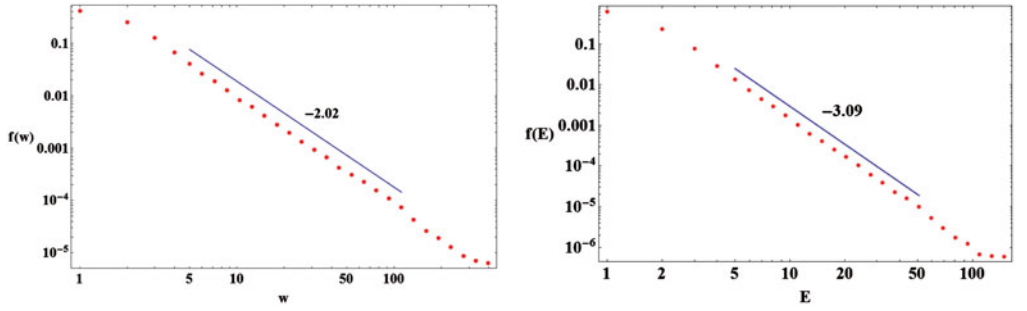

FIGURE 6. The figure, from Berger and Asgari-Targhi (2009), shows the distribution of braid sequence sizes and flare energies for a zero net helicity braid. Here the braids start with 1000 sequences, with equal probability of positive and negative sequences. The braids undergo reconnections; same sign sequences merge while opposite sign sequences cancel or partially cancel. The braids maintain their size by new sequences inserted at the boundaries.

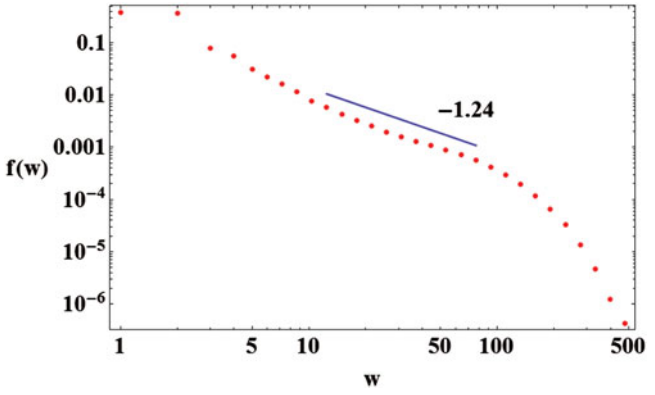

FIGURE 7. This simulation presents results for braids with a bias towards positive sequences. Here 60% of the sequences will on average be positive. While the sequence distributions flattened somewhat, there were very few flares of any significant energy, as cancellations were rare.

However, one might argue that there could be a bias toward sequences of one sign (Karpen et al. 1993). In Fig. 7 we demonstrate the power law fit for a braid with, on average, 60% positive coherent sequences. If there are more positive braid crossings than negative braid crossings, then the magnetic helicity will be positive. The number of larger sequences rises, as there will be more mergers; but correspondingly there are much fewer cancellations of sequences of opposite sign.

Thus in this simple model, net helicity suppresses energy release. In a more involved model, hundreds of strands could be included in the braid, as well as internal twist. Neighbouring flux of like twist can merge due to reconnection, resulting in a release of energy (Wilmot-Smith et al. 2011). Thus, the presence of net twist can in fact prove avenues of energy release not yet included in the discrete braid model.

4. Discussion and conclusion

Numerical simulations of magnetic braiding (e.g. (Rappazzo et al. 2007; Wilmot-Smith et al. 2011)) have employed smooth flux distributions at the boundaries.

https://doi.org/10.1017/S0022377815000483 Published online by Cambridge University Press

Multiple thin current layers soon form throughout the volume, leading to rapid dissipation of the braid structure.

However, the photospheric magnetic field appears in discrete flux elements. It is possible that this discreteness will enhance both the amount of braid structure entering the corona from the photosphere, as well as the amount of braid structure the corona can hold.

First, the input of braid structure by footpoint motions will be more efficient if the flux moves in discrete pieces. A smoothly varying velocity field will braid some field lines more than others, if the field lines are distributed smoothly through the boundary. Secondly, for the discrete case, current sheets will certainly form between strands, but they will not appear within strands. Thus, the strong currents will not be as ubiquitous as in the continuous models. In the Parker scenario, the current sheets between strands slowly burn until a secondary instability sets off a reconnection event, hence a nanoflare (Parker 1972; Dahlburg et al. 2005).

This paper has investigated the braiding structure of coronal loops generated by discrete footpoint motions. We have shown, using a simple forest fire model, that structure in the direction along the braid can become self-organized due to selective reconnection. Power laws result, but these are steeper than expected from observations. The model presented here is essentially one-dimensional as the self-organization occurs only in the direction parallel to the loop axis. A more involved model would include self-organization in the transverse directions. This can be done by including a high number of strands, and going beyond braid theory to include internal twist.

Acknowledgement

M. Berger is happy to thank the Leverhulme Trust grant SH-04409 which helped support this research. M. Asgari-Targhi and E.E. DeLuca are supported by the AIA contract SP02H1701R.

REFERENCES

Artin, E. 1947 *Ann. Math.* **48**, 101.

Aschwanden, M. J. 2004 *Physics of the Solar Corona. An Introduction.* Praxis Publishing Ltd., Chichester, UK: Springer-Verlag Berlin.

Aschwanden, M. J. 2013 *Self-Organized Criticality Systems.* Berlin Warsaw: Open Academic Press.

Asgari-Targhi, M., Schmelz, J. T., Imada, S., Pathak, S. and Christian, G. M. 2015, Submitted to *Astrophys. J.*

Asgari-Targhi, M. and van Ballegooijen, A. A. 2012 *Astrophys. J.* **746**, 81.

Asgari-Targhi, M., van Ballegooijen, A. A., Cranmer, S. R. and DeLuca, E. E. 2013 *Astrophys. J.* **773**, 111.

Asgari-Targhi, M., van Ballegooijen, A. A. and Imada, S. 2013 *Astrophys. J.* **786**, 28.

Babcock, K. L. and Westervelt, R. M. 1990 *Phys. Rev. Lett.* **64**, 2168.

Bak, P., Tang, C. and Wiesenfeld, K. 1987 *Phys. Rev. Lett.* **59**, 381.

Bak, P., Tang, C. and Wiesenfeld, K. 1988 *Phys. Rev.* A **38**, 364.

Berger, M. A. 1990 Third-order invariants of randomly braided curves. In: *Topological Fluid Mechanics*, (ed. H. K. Moffatt and A. Tsinober). Cambridge: Cambridge University Press, pp. 440–448.

Berger, M. A. 1993 *Phys. Rev. Lett.* **70**, 705.

Berger, M. A. 1994 *Space Sci. Rev.* **68**, 3.

Berger, M. A. and Asgari-Targhi, M. 2009 *Astrophys. J.* **705**, 347.

Berger, T. E. and Title, A. M. 1996 *Astrophys. J.* **463**, 365

https://doi.org/10.1017/S0022377815000483 Published online by Cambridge University Press

Carlson, J. M. and Langer, J. S. 1989 *Phys. Rev. Lett*. **62**, 2632.
Cargill, P. J. and Klimchuk, J. A. 1997 *Astrophys. J*. **478**, 799.
Charbonneau, P., McIntosh, S., Liu, H. and Bogdan, T. 2001 *Sol. Phys*. **203**, 321.
Cirtain, J. W., Golub, L., Winebarger, A. R. et al. 2013 *Nature* **493**, 501.
Craig, I. J. D. 2010 *Sol. Phys*.**266**, 293.
Dahlburg, R. B., Klimchuk, J. A. and Antiochos, S. K. 2005 *Astrophys. J*. **622**, 1191.
Datlowe, D. W., Elcan, M. J. and Hudson, H. S. 1974 *Sol. Phys*. **39**, 155.
Dennis, B. R. 1985 *Sol. Phys*. **100**, 465.
Einaudi, G. and Velli, M. 1999 *Phys. Plasmas* **6**, 4146.
Galloway, R. K., Helander, P. and MacKinnon, A. L. 2006 *Astrophys. J*. **646**, 615.
Golub, L. and Pasachoff, J. M. 2009 *The Solar Corona*. Cambridge: Cambridge University Press.
Ionson, J. A. 1985 *Sol. Phys*.**100**, 289.
Ionson, J. A. and Hudson, H. S. 2010 *Nature Phys*. **6**, 637.
Janse, Å. M. and Low, B. C. 2009 *Astrophys. J*. **690**, 1089.
Janse, Å. M., Low, B. C. and Parker, E. N. 2010 *Phys. Plasmas* **17**, 092 901.
Kadanoff, L., Nagel, S. R., Wu, L. and Zhou, S. 1989 *Phys. Rev*. A **39**, 6524.
Karpen, J. T., Antiochos, S. K., Dahlburg, R. B. and Spicer, D. S. 1993 *Astrophys. J*. **403**, 769.
Klimchuk, J. A., Patsourakos, S. and Cargill, P. J. 2008 *Astrophys. J*. **628**, 1351.
Lin, R. P., Schwartz, R. A., Kane, S. R., Pelling, R. M. and Hurley, K. C. 1984 *Astrophys. J*. **283**, 421.
Linton, M. G., Dahlburg, R. B. and Antiochos, S. K. 2001 *Astrophys. J*. **553**, 905.
Longcope, D. and Strauss, H. 1994 *Sol. Phys*.**149**, 63.
Low, B. C. 2010 *Sol. Phys*.**266**, 277.
Lu, E. T. and Hamilton, R. J. 1991 *Astrophys. J*. **380**, L89.
Mandrini, C. H., Démoulin, P. and Klimchuk, J. A. 2000 *Astrophys. J*. **530**, 999.
Milano, L. J., Gómez, D. O. and Martens, P. C. H. 1997 *Astrophys. J*. **490**, 442.
Ng, C. S. and Bhattacharjee, A. 1998 *Phys. Plasmas* **5**, 4028.
Parker, E. N. 1972 *Astrophys. J*. **174**, 499.
Parker, E. N. 1983 *Astrophys. J*. **264**, 642.
Parker, E. N. 1988 *Astrophys. J*. **330**, 474.
Patsourakos, S. and Klimchuk, J. A. 2006 *Astrophys. J*. **647**, 1452.
Priest, E. R., Heyvaerts, J. F. and Title, A. M. 2002 *Astrophys. J*. **576**, 533.
Rappazzo, A. F., Velli, M., Einaudi, G. and Dahlburg, R. B. 2007 *Astrophys. J. Lett*. **657**, L47.
Rappazzo, A. F., Velli, M., Einaudi, G. and Dahlburg, R. B. 2008 *Astrophys. J*. **677**, 1348.
Reep, J. W., Bradshaw, S. J. and Klimchuk, J. A. 2013 *Astrophys. J*. **746**, 193
Schrijver, C. J. 2007 *Astrophys. J*. **662**, L119.
Schrijver, C. J. and Zwaan, C. 2000 *Solar and Stellar Magnetic Activity*. Cambridge: Cambridge University Press.
Shibata K. et al. 2007 *Science* **318**, 1591.
Song, Y. and Lysak, R. L. 1989 *J. Geophys. Res-Space Phys*. **94**, 5273–5281.
van Ballegooijen, A. A. 1986 *Astrophys. J*. **311**, 1001.
van Ballegooijen, A. A., Asgari-Targhi, M. and Berger, M. A. 2014 *Astrophys. J*. **787**, 87.
van Ballegooijen, A. A., Asgari-Targhi, M., Cranmer, S. R. and DeLuca, E. E. 2011 *Astrophys. J*. **736**, 3.
Verdini, A. and Velli, M. 2007 *Astrophys. J*. **662**, 669.
Vlahos, L., Georgoulis, M., Kluiving, R. and Paschos, P. 1995 *Astron. Astrophys*. **299**, 897.
Wilmot-Smith, A. L., Hornig, G. and Pontin, D. I. 2009 *Astrophys. J*. **704**, 1288.
Wilmot-Smith, A. L., Pontin, D. I., Yeates, A. R. and Hornig, G. 2011 *Astron. Astrophys*. **536**, A67.
Winebarger, A. R. and Warren, H. P. 2005 *Astrophys. J*. **626**, 543.
Wright, A. and Berger, M. A. 1989 *J. Geophys. Res*. **94**, 1295.

https://doi.org/10.1017/S0022377815000483 Published online by Cambridge University Press